Lipid Phase Dependence of DNA−Cationic Phospholipid Bilayer Interactions Examined Using Atomic Force Microscopy

Zoya V. Leonenko,[†] Dennis Merkle,[†,‡,§] Susan P. Lees-Miller,[‡,§] and David T. Cramb*[,†]

Departments of Chemistry and Biological Sciences, University of Calgary, 2500 University Drive NW, Calgary, AB T2N 1N4 Canada, and Department of Biochemistry and Molecular Biology, 3300 Hospital Drive NW, University of Calgary, T2N 4N1 Canada

Received October 31, 2001. In Final Form: February 20, 2002

Magnetic AC mode atomic force microscopy was used to study DNA adsorption onto supported cationic phospholipid (CL) bilayers in the fluid (L_α) and gel (L_β) phases. A L_α phase CL bilayer was used as a model system to study DNA−CL complex formation at the single molecule level. Pure and mixed bilayers of dioleoyltrimethylammonium propane (DOTAP), dioleoylphosphatidylethanolamine (DOPE), dioleoylphosphatidylcholine (DOPC), and dipalmitoyltrimethylammonium propane (DPTAP) were investigated. The adsorption of small oligodeoxynucleotide DNA (14 base pairs) and large (1000−3000 base pairs) was examined and revealed that the behavior of the DNA−CL complex depends on the length and density of DNA. Once adsorbed to the bilayer, large DNA induced changes in the bilayer coverage of the mica support, while short DNA did not destabilize the bilayer. There was a strong dependence of the bilayer destabilization on the type of neutral helper lipid mixed with the cationic lipid, with DOTAP/DOPE being much less stable to DNA adsorption than DOTAP/DOPC. The characteristics of pure and mixed DOTAP, DOPE, and DOPC supported phospholipid bilayers were investigated to understand the stability changes induced by DNA. Images of the DNA-free phospholipid bilayer revealed the dependence of supported planar bilayer structure and stability on the chemical nature of the headgroup and on the phase of the bilayer. Finally, it was illuminating to image DNA on DPTAP bilayers as a function of temperature. When the system was examined above the L_α−L_β phase transition, images similar to those recorded for DNA−DOTAP (L_α) and DNA−DOTAP/DOPC (L_α) were observed.

Introduction

Cationic lipids are capable of delivering both hydrophobic and hydrophilic compounds[1] to the cell. They are effective in vitro[2] and in vivo.[3] There are several advantages to using liposomes over other drug delivery systems: Phospholipids are expected to be nontoxic, because they are natural constituents of all cell membranes; drugs encapsulated within a liposome are protected from the environment, which prevents enzymatic degradation;[4] they limit immunogenic problems associated with viral gene delivery, are simple to prepare, and can carry DNA of reasonably large size.[5]

The process of gene delivery includes lipoplex formation between DNA and cationic lipids, with the DNA−cationic phospholipid (CL) lipoplex then promoting vector delivery through the cell membrane to the nucleus. The mechanism by which genetic material is delivered to the nucleus is not entirely clear. Moreover, despite their promise as gene transfer reagents, the phase dependence of DNA−cationic lipid interactions has not been extensively studied at the single molecule level. Commonly, liposomes used for complex formation consist of a binary mixture of cationic lipids and neutral helper lipids (HL). The helper lipids (e.g., dioleoylphosphatidylethanolamine (DOPE)) enhance vesicle fusogenicity. The formation and stability of the lipoplexes depend on many factors, examples of which are the type of HL,[6] the solvent environment, and the order of mixing DNA and lipids in lipoplex preparation.[7] The type of HL employed has been shown to affect the structure of complexes and the transfection efficiency.[8,9]

Several recent studies have investigated phospholipid−DNA interactions[7,10−16] in solution. The lipoplex structures resulting from DNA−CL interactions in solution (DNA interactions with vesicles) can be divided into five types. The first is a DNA−monolayer phospholipid interaction

* Corresponding author. E-mail: dcramb@ucalgary.ca.
[†] Department of Chemistry.
[‡] Department of Biological Sciences.
[§] Department of Biochemistry and Molecular Biology.

(1) Knight, C. G. Hydrophobic pro-drugs in liposomes. In *Liposomes: from physical structures to therapeutic applications*; Knight, C. G., Ed.; Elsevier/North Holland Biomedical Press: Amsterdam, 1981; pp 381−390.
(2) Felgner, P. L.; Gadek, T. R.; Holm, M.; Roman, R.; Chan, H. W.; Wenz, M.; Ringold, J. P.; Danielsen, M. *Proc. Natl. Acad. Sci. U.S.A.* **1987**, *84*, 7413−7417.
(3) Templeton, N. S.; Lasi, D. D.; Frederic, P. M.; Strey, H. H.; Roberts, D. D.; Palvakis, G. N. *Nat. Biotechnol.* **1997**, *15*, 647−652.
(4) Sorgi, F. L.; Huang, L. Drug delivery applications. In *Current Topics in Membranes*; 1997; pp 44, 449−474.
(5) Signhal, A.; Huang, L. In *Gene therapy*; Hui, K. M., Ed.; World Scientific: New York, 1994; Chapter 6.
(6) May, S.; Harris, D.; Ben-Shaul, A. *Biophys. J.* **2000**, *78*, 1681−1697.
(7) Kennedy, M. T.; Pozharski, E. V.; Rakhmanova, V. A.; MacDonald, R. C. *Biophys. J.* **2000**, *78*, 1620−1633.
(8) Hui, S. W.; Langner, M.; Zhao, Y.-L.; Patrick, R.; Hurley, E.; Chan, K. *Biophys. J.* **1996**, *71*, 590−599.
(9) Zuidam, N. J.; Lerner, D. H.; Margulies, S.; Barenholz, Y. *Biochim. Biophys. Acta* **1999**, *1419*, 207−220.
(10) Koltover, I.; Salditt, T.; Rädler, J. O.; Safinya, C. R. *Science* **1998**, *281*, 78−81.
(11) Rädler, J. O.; Koltover, I.; Jamieson, A.; Salditt, T.; Safinya, C. R. *Langmuir* **1998**, *14*, 4272−4283.
(12) Wong, F. M. P.; Reimer, D. L.; Bally, M. B. *Biochemistry* **1996**, *35*, 5756−5763.
(13) May, S.; Ben-Shaul, A. *Biophys. J.* **1997**, *73*, 2427−2440.
(14) Dan, N. *Biochim. Biophys. Acta* **1998**, *1369*, 34−38.
(15) Wagner, K.; Harries, D.; May, S.; Kahl, V.; Radler, J. O.; Ben-Shaul, A. *Langmuir* **2000**, *16*, 303−306.
(16) Dan, N. *Biophys. J.* **1997**, *73*, 1842−1846.

10.1021/la0116239 CCC: $22.00
Published on Web 04/05/2002

where a phospholipid monolayer wraps around the double-stranded DNA. This complex is hydrophobic and exists in the form of an inverted tubular micellelike structure. It has been shown[12] that the formation of such a hydrophobic complex can transfer a hydrophilic DNA molecule from the aqueous phase to an organic phase. The next four lipoplexes involve lipid bilayers. The first of these may be described as a *beads on a string* complex, where liposomes adhere to the DNA. This structure is rarely observed. The next is a cylindrical complex, where a single DNA strand is surrounded by phospholipid bilayer.[13,14] A more common structure is a condensed lamellar CL−DNA complex, where DNA intercalates liposome bilayers in a locally flat lamellar structure.[11,15,16] This structure is most stable when the cationic and helper lipids have small spontaneous curvatures and where the lipoplex is nearly charge neutral.[6,10,11] Lipids typical of this behavior in spontaneous curvature are dioleoyltrimethylammonium propane (DOTAP) (CL) and dioleoylphosphatidylcholine (DOPC) (HL), respectively. Finally, when the helper lipid has a large, often negative, spontaneous curvature, a honeycomb complex occurs.[13,17] DOPE as a helper lipid is a classic promoter of inverted hexagonally packed honeycomb lipoplexes.[10]

Much of the previous work examining DNA−CL lipoplexes has employed either X-ray scattering[10,18,19] or fluorescence.[20−25] Furthermore, DNA−bilayer interactions have been studied mostly in solution. However, atomic force microscopy (AFM) can be a powerful tool to study DNA interaction and complex formation at the surface of a supported phospholipid bilayer. There have been only a few studies using AFM to examine DNA on supported cationic bilayers. To date, these attempts have been successful only for L_β phase bilayers. In 1995, Mou et al.[26] measured the double helix pitch of DNA adsorbed onto dipalmitoyltrimethylammonium propane (DPTAP). They found that ethylenediaminetetraacetic acid (EDTA) was essential for enhancing the close packing of DNA. In 1997, a study by Fang and Yang[27] concluded that the adsorption−condensation mechanism of both linear and circular forms of DNA onto cationic supported dipalmitoyldimethylammoniumylpropane (DPDAP) or distearoyldimethylammoniumylpropane (DSDAP) bilayers involves tight two-dimensional packing of DNA on the bilayer surface. AFM images displayed closely packed DNA adsorbed onto the L_β phase supported bilayer, showing cooperative electrostatic interactions rather than random adsorption. A third study examined the interaction of DNA with supported planar L_β bilayers of DPTAP, dimethyldioctadecylammonium bromide (DODAB), and DOTAP[28] in order to determine the effect of surface charge density on DNA packing efficiency. The L_β phase bilayers of DPTAP and DODAB provided excellent contrast in the AFM images of adsorbed DNA. However, the authors could not detect DNA on pure DOTAP, citing a possibly high lateral DNA mobility of the L_α phase bilayer. We have recently shown that DNA may induce lipid demixing in a DPTAP/DPPE supported planar bilayer (SPB) when the system is raised above the L_α−L_β phase transition.[29]

In the present work, we investigate DNA−CL lipoplex formation by using a L_α phase supported bilayer to model the lipoplex system, rather than using vesicles in solution, because we hoped to follow the first steps of complex formation. There is considerable challenge in using AFM to study DNA on supported planar bilayers in the liquid L_α phase. In addition to lateral mobility concerns, image contrast will be limited by penetration of DNA into the soft bilayer. This penetration could be either a natural embedding or tip induced. Tip bilayer penetration has recently been addressed for contact mode imaging of pure bilayers.[30] The challenge for AFM measurements of DNA on liquid bilayer surfaces is akin to using one's finger for sensing wet spaghetti held on top of water by surface tension. Moreover, addition of the helper lipid DOPE increases the instability of the bilayer.[8] Such mixed bilayer systems are challenging for current AFM technology, since they are soft and dynamic. However, because of their ease of deformation, L_α phase bilayers must be very sensitive to the presence of DNA and may easily respond to perturbations caused by adsorbed DNA. In a previous study, we have shown magnetic AC (MAC) tapping mode AFM to be very sensitive to L_α phase DOPC bilayer dynamics, while remaining minimally invasive.[31] Thus, it was anticipated that MAC mode AFM would enable the collection of AFM images to help elucidate DNA−CL structure and dynamics when the lipid bilayer is in its L_α state.

In this study, we used MAC mode AFM to examine the interactions of DNA with supported DOTAP, DOTAP/DOPE, DOTAP/DOPC, and DPTAP bilayers on a mica support in an aqueous environment. The SPBs were formed using the vesicle fusion method. When DNA was added to the fluid cell, it was observed to adsorb to the bilayer. The dependence of the DNA−CL lipoplex structure and stability on the phospholipid headgroup and on the size of DNA was explored. We found that short oligonucleotides formed very stable supported lipoplexes, whereas longer linear DNA (1000−3000 base pair) induced considerable change in the bilayer. This DNA-induced change ranged from bilayer thickening, to rupture, to removing the bilayer from the mica surface. A L_β phase DPTAP bilayer, used for comparison, produced a more stable DNA−bilayer complex at room temperature and higher contrast/resolution AFM images. By inducing a transition of the bilayer from L_β phase to L_α phase ($T_{L_\beta-L_\alpha}$ = 45 °C)[32] at 50 °C, we found that the AFM image contrast/resolution of adsorbed DNA was lowered. Additionally, by comparing these images with the pure bilayer images above and below the L_β−L_α phase transition, we can conclude that the degradation of the image is due to the increase in bilayer fluidity and not due to temperature-induced tip effects.

(17) Harries, D.; May, S.; Gelbart, W. M.; Ben-Shaul, A. *Biophys. J.* **1998**, *75*, 159−173.
(18) Koltover, I. T.; Wagner, K.; Safinya, C. R. *Proc. Natl. Acad. Sci. U.S.A.* **2000**, *97*, 14046−14051.
(19) Rädler, J. O.; Koltover, I.; Salditt, T.; Safinya, C. R. *Science* **1997**, *275*, 810−814.
(20) Lam, A. M. T.; Cullis, P. R. *Biochim. Biophys. Acta* **2000**, *1463*, 279−290.
(21) Meiden, V. M.; Cohen, J. C.; Amariglio, N.; Hirsch-Lerner, D.; Barenholz, Y. *Biochim. Biophys. Acta* **2000**, *1464*, 251−261.
(22) Even-Chen, S.; Barenholz, Y. *Biochim. Biophys. Acta* **2000**, *1509*, 176−181.
(23) Son, K. K.; Patel, D. H.; Tkach, D.; Park, A. *Biochim. Biophys. Acta* **2000**, *1466*, 11−15.
(24) Harvie, P.; Wong, F. M. P.; Bally, M. B. *Biophys. J.* **1998**, *75*, 1040−1051.
(25) Zelphati, O.; Szoka, F. C. *Proc. Natl. Acad. Sci. U.S.A.* **1996**, *93*, 11493−11498.
(26) Mou, J.; Czajkowsky, D. M.; Zhang, Y.; Shao, Z. *FEBS Lett.* **1995**, *371*, 279−282.
(27) Fang, Y.; Yang, J. *J. Phys. Chem. B* **1997**, *101*, 441−449.
(28) Clausen-Schaumann, H.; Gaub, H. E. *Langmuir* **1999**, *15*, 8246−8251.
(29) Leonenko, Z.; Cramb, D. *Nano Lett.* **2002**, in press.
(30) Schneider, J.; Dufrêne, Y. F.; Barger, W. R., Jr.; Lee, G. U. *Biophys. J.* **2000**, *79*, 1107−1118.
(31) Leonenko, Z. V.; Carnini, A.; Cramb, D. T. *Biochim. Biophys. Acta* **2000**, *1509*, 134−147.
(32) McKiernan, A. E.; Ratto, T. V.; Longo, M. L. *Biophys. J.* **2000**, *79*, 2605−2615.

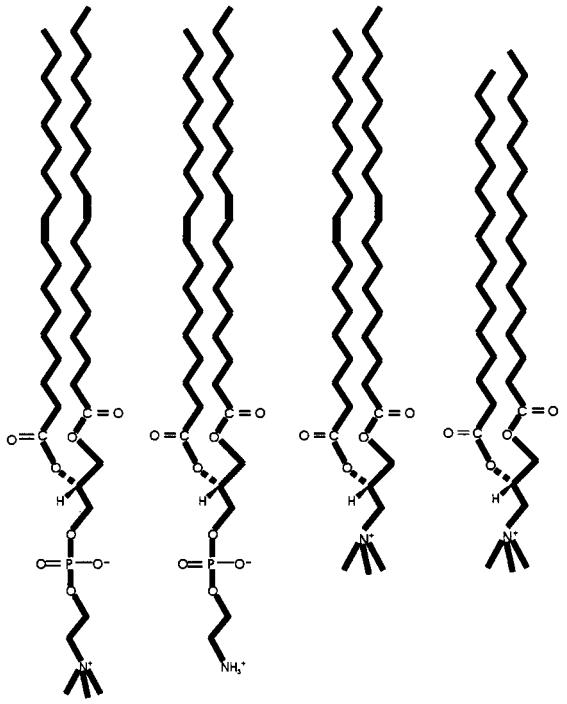

Figure 1. The structures of DOPC, DOTAP, DOPE, and DPTAP.

Materials and Methods

Materials. DOPC (lyophilized or in chloroform solution) (Sigma, Oakville, ON), DOPE, DOTAP (chloroform solution), and DPTAP (Avanti Polar Lipids Inc., Alabaster, AL) were used without further purification. Structures of the phospholipids are displayed in Figure 1. The 14 base pair oligonucleotide (ATATAAATTTATAT) was obtained desalted from UCDNA services (University of Calgary, AB). The longer 1000 base pair DNA was calf thymus (Sigma), type II, fragmented by ultrasonication. The 2880 base pair, pTZ 18U closed circular supercoiled plasmid DNA (Sigma) was used as received. Three thousand base pair, linearized plasmid DNA was prepared according to standard procedures.[33] B-GAL linear DNA, 3000 base pairs, was a gift from the Biotechnology Laboratory of the University of Calgary. Tris-EDTA (TE) buffer (pH = 7.6) and distilled, ultrapure water were used in the generation of all vesicles. Freshly cleaved mica or chemically modified mica was used throughout this study as a substrate. A positively charged mica surface was required to bind polyanionic DNA. This was created by adding a dilute solution of either 3-aminopropyltriethoxy-silane (APTES) or poly-L-lysine (PLL) (Sigma) onto the mica surface. After 2−5 min, the mica was rinsed with ultrapure water and dried with nitrogen. Freshly cleaved mica, which carries a slightly negative charge in H_2O,[34] was found to bind cationic liposomes, and therefore no surface modification was necessary.

Vesicle and Supported Planar Bilayer Preparation. All vesicles were prepared using the "dry" method as previously reported.[31] The binding of DNA to the vesicles was performed by stirring DNA with a vesicle solution. Supported planar bilayers were prepared for AFM imaging by the method of vesicle fusion.[35] Aliquots of liposome solution were deposited on modified or unmodified freshly cleaved ASTMV-2 quality, scratch-free ruby mica (Asheville-Schoonmaker Mica Co., Newport News, VA). After a controlled period of time, the mica was gently rinsed with ultrapure water. Solutions of DNA (10−200 μL, 10−2000 μg/mL) were pipetted onto the wet phospholipid bilayer surface and were left to incubate at 4 °C for 1−24 h. The excess DNA was gently rinsed away, and the surface was imaged under water in the liquid cell, at room temperature and at various higher temperatures.

Atomic Force Microscopy. AFM is a surface imaging technique with nanometer-scale lateral resolution and angstrom normal resolution, which operates by measuring the forces acting between a probe and a sample. We employed MAC (magnetic AC) mode,[36,37] where a magnetically coated probe oscillates near its resonant frequency driven by an alternating magnetic field. This technique has proven to be advantageous for measuring supported planar bilayers in liquid media.[31] All images were taken using a Pico SPM with an AFMS-165 scanner (Molecular Imaging Inc., Phoenix, AZ). Au−Cr coated Maclevers (Molecular Imaging Inc.) were used for MAC mode imaging. Their specifications include a length of 85 μm, a force constant of 0.06−0.1 N/m, and a resonant frequency of 20−40 kHz in liquid. The standard MAC mode fluid cell (Molecular Imaging) was used throughout. The scanning speed was 1−2 lines per second. The height scale was calibrated using colloidal gold spheres of 5 nm in diameter.[38] For elevated temperature experiments, the AFM Temperature Controller and Hot Mac Mode Stage from Molecular Imaging Inc. were used.

Statistics. The mean value(s) of DNA height(s) and bilayer thickness were calculated using between 40 and 100 measurements over several scanned regions, where appropriate. The standard deviation is quoted at the 99% confidence level.

Results and Discussion

The lipid composition of natural membranes plays an important role in membrane function,[39] especially when the membrane is close to a $L_\alpha-H_{II}$ phase transition. Important examples where the lipid phase is critical are membrane fusogenity and the process of DNA transfection. The bending modulus and the intrinsic radius of curvature are two characteristics of the state of a lipid in a planar bilayer that affect the outcome of interactions with DNA.[6] In the following, we discuss how the above phenomena affect supported planar bilayer formation and the formation of SPB−DNA complexes.

To assess the effect of DNA adsorption to the L_α phase SPBs, pure DOTAP, DOPC, and DOPE and mixed phospholipid bilayers supported on mica and modified mica surfaces were investigated first. The evaluation of these bilayers is of considerable interest, because they differ only in headgroup (Figure 1). All of the L_α phase bilayers developed bilayer defects, as was previously observed for DOPC.[31] Thus, their thickness and fluidity could be assessed using AFM by observing defect depth and mobility, respectively. DPTAP bilayers were examined to compare their L_β phase and L_α phase interactions with DNA. The DNA samples used to create the lipoplexes were also imaged in the absence of SPBs in order to compare their heights to those determined when adsorbed to the cationic SPBs.

Supported Phospholipid Bilayers. *DOPC Bilayer.* DOPC bilayers formed from vesicle solution in acetate or TE buffer (pH = 7.6) or in pure water show good coverage of the surface with only a few defects apparent. Consistent with our previous study,[31] slow defect changes were observed. The DOPC bilayer thickness is 5.8 ± 0.1 nm, when the bilayer was formed from acetate buffer solution.

(33) Sambrook, J.; Fritsch, E. F.; Maniatis, T. *Molecular Cloning*: *A Laboratory Manual*; Cold Spring Harbor Publications: Cold Spring, NY, 1989.
(34) Muller, D. J.; Amrein, M.; Engel, A. *J. Struct. Biol.* **1997**, *119*, 172−188.
(35) Brian, A. A.; McConnell, H. M. *Proc. Natl. Acad. Sci. U.S.A.* **1984**, *81*, 6159−6163.
(36) Han, W.; Lindsay, S. M.; Jing, T. *Appl. Phys. Lett.* **1996**, *69*, 1−3.
(37) Han, W.; Lindsay, S. M. *Appl. Phys. Lett.* **1998**, *72*, 1656−1658.
(38) Vesenka, J.; Manne, S.; Giberson, R.; Marsh, T.; Henderson, E. *Biophys. J.* **1993**, *65*, 992−997.
(39) Epand, R. M.; Fuller, N.; Rand, R. P. *Biophys. J.* **1996**, *71*, 1806−1810.

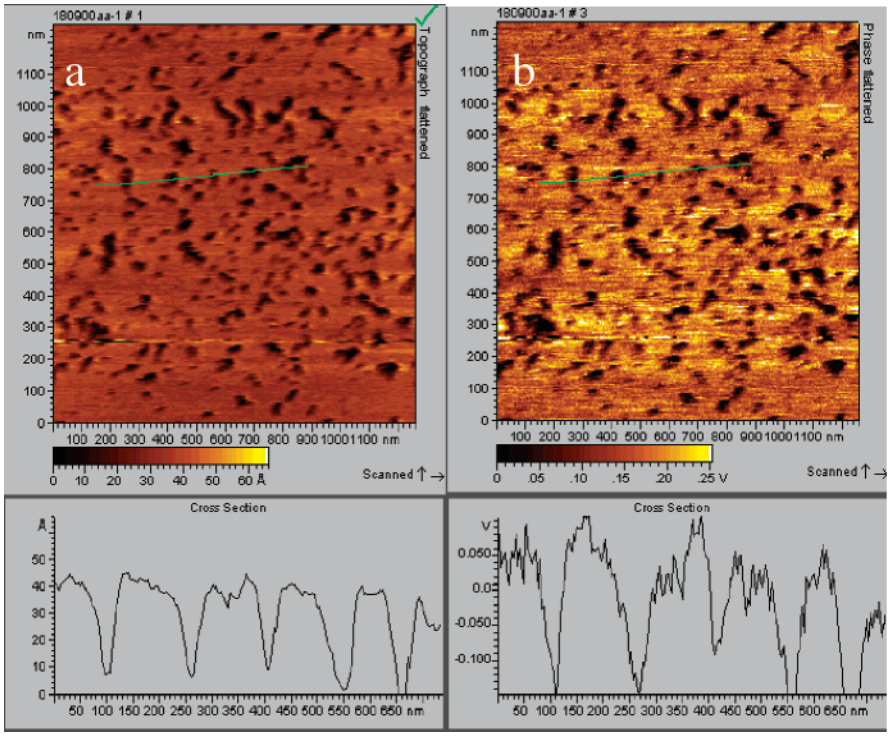

Figure 2. An AFM image of a DOTAP supported planar bilayer on mica imaged in water. The images are approximately 700 nm × 700 nm. Panel a is topography, and panel b is a phase image, recorded simultaneously. The subpanels are cross sections indicated by the green lines in the main panels. Dark areas in panel a are defects in the supported planar bilayers. The phase difference across the defect indicates that it is a different material (mica) than the higher features (DOTAP bilayer).

Table 1. Properties of Supported Planar Bilayers

phospholipid(s)	when formed in TE buffer (nm)	when formed in water (nm)	literature data bilayer thickness (nm)[a]	defect closing time
DOTAP	3.5	3.7	3.7	<1 h
DOPE	4.5	2.7		<1 h (H_2O) >3 h (TE)
DOPC	5.4	5.4	4.2	>3 h
DOTAP/DOPC	4.7	4.9	3.9	>3 h
DOTAP/DOPE	2.4	2.9		<1 h
DPTAP	5.5/3.8[b]		4.1/2.7[c]	none

[a] Data from ref 11. [b] The bilayer had domains of two different heights. [c] Data from ref 40.

The thickness of the DOPC bilayer is 5.4 ± 0.3 nm when it is formed from vesicle solution in TE buffer and 5.4 ± 0.2 nm when the bilayer is formed from vesicle solution in pure water (Table 1). The thicknesses of the DOPC bilayer in water and TE buffer are virtually identical at 5.4 nm. This compares favorably with our previous study where the fusion of DOPC vesicles from acetate buffer produced a bilayer 5.8 nm thick[31] (Table 1). DOPC is well modeled as a cylinder, making the lamellar phase most stable at room temperature.

DOTAP Bilayer. Supported DOTAP bilayers were formed on regular freshly cleaved mica by applying 70 μL of 0.2 mg/mL vesicle solution in water. After 10 min, the liquid cell was gently rinsed with water. SPBs were always imaged in an aqueous environment. By an average over several regions, the bilayer thickness was determined as 3.7 ± 0.2 nm. A TE buffer (pH = 7.6) vesicle solution exposed to the mica for 10 min did not lead to SPB formation. Increasing the incubation time to 1 h, however, did promote SPB formation. In this case, the thickness of the bilayer was 3.5 ± 0.1 nm. The topographical and phase images of a DOTAP SPB are presented in parts a and b of Figure 2, respectively. As with our previous study of DOPC,[31] the phase image convinces us that the defects are holes in the bilayer with exposed mica at their bottoms, because of the stark phase contrast over these features. The fluidity of the DOTAP bilayer was relatively high, with the major defects closing in less than 1 h, leaving only the small-scale defects observed in Figure 2. The SPB thickness did not change during bilayer spreading. This is likely because equilibration takes place between highly stressed dense areas of the bilayer (which could be created during vesicle fusion) and relaxed areas of the bilayer. The apparent filling of defects by DOTAP (see Figure 2) could arise from an increase in the average area per phospholipid as the bilayer relaxes. In the original vesicles, the area per DOTAP may be restricted by the vesicle dimensions. Consistent with the present study, high fluidity DOTAP and other charged phospholipid supported bilayers were observed previously.[40,41]

The fact that the thickness of a pure DOTAP SPB is not significantly affected by changing contents of the aqueous solution is in good agreement with the concept that methyl group screening limits the effect of hydration on headgroup volume, as in DOPC. The difference in the bilayer thickness of pure DOTAP and DOPC is likely attributable to the different headgroup charges, volumes, and geometries, since the hydrophobic tails are identical. The distances between the adjacent headgroups of DOTAP are effectively larger than those of DOPC due to Coulombic repulsion between their positive charges. The larger headgroup area would promote gauche defects leading to bilayer compression due to an increase in the hydrocarbon chain disorder, possibly involving tail interdigitation. Indeed, hydrocarbon chain disorder, such as tilting and interdigitation, has been cited as the cause of bilayer thinning, observed using AFM.[10,32,42,43] This suggests that

(40) Schouten, S.; Stroeve, P.; Longo, M. L. *Langmuir* **1999**, *15*, 8133–8139.
(41) Zhang, L.; Sroeve, P.; Longo, M. L. *Langmuir* **2000**, *16*, 5093–5099.

a change in the bilayer thickness can be induced by lateral swelling of the bilayer. Thinner bilayers can also result from mica−bilayer interactions (the water layer between mica and bilayer may vary in thickness) and electrostatic tip−bilayer interactions. We believe that the mica−bilayer interaction and electrostatic tip−bilayer interactions are small. The water layer is usually 1−2 nm,[44] and changes in the water layer thickness cannot decrease the thickness of the bilayer lower than double the length of the phospholipid molecule. The charge of the tip is negligible in water, and imaging charged species such as DNA does not produce errors (DNA height on a solid support gives 2 nm, which is in agreement with the real DNA diameter[11]). Therefore, the major differences in the bilayer thickness can be attributed to disorder increase in the bilayer. Although we observe thinner bilayers under certain conditions, from AFM images alone it is not possible to know the mechanism with absolute certainty.

DOPE Bilayer. Our results indicate that the stable formation of supported planar bilayers for pure DOPE is possible via vesicle fusion, provided that a low enough concentration (0.1 mg/mL) of lipid is used in the preparation of the vesicles. At low concentrations and short exposure times, we observe circular areas with the thickness of a single bilayer, Figure 3a. This is highly suggestive that either small unilamellar liposomes or bilayer fragments existed in the sonicated aqueous solutions used for vesicle fusion.[31] Also found in Figure 3a are small regions of continuous bilayer. The thickness of the bilayer is 4.5 ± 0.1 nm. The supported bilayer is stable in time, showing no defect dynamics during the time of observation (2−3 h). At higher DOPE concentrations (>0.1 mg/mL), we observe the coexistence of a bilayer and aggregates on the mica surface, see Figure 3b. The ordered structures in Figure 3b found in the aggregates could represent a hexagonal phase. The striations observed in Figure 3b (see arrows) have a spacing of about 10 nm. This is slightly larger than the measured repeat distance of 6.5 nm measured by Epand et al.[39] using diffraction techniques. The larger distance could result from electrostatic interactions with the mica support. Alternatively, these features are quite reminiscent of electron microscopy images where a ripple phase is present.[45] However, the ripple phase has previously been observed only for saturated lipids with phosphatidylcholine and phosphatidylglycerol headgroups. We believe that the 10 nm striations are not artifacts because they appear to have different orientations relative to the scan direction as noted by the two arrows.

Although the H_{II} phase is reputed to be the most stable for DOPE in pH-neutral aqueous solution at room temperature,[46] we found that a DOPE solution in water (up to 5 mg/mL) clarified when sonicated. This suggests that small aggregates and possibly vesicles are present. When adsorbed to regular mica from pure water, DOPE forms extended regions of bilayer coverage. Here, the bilayer was observed to be very fluid, with the defects closing in a maximum of 1 h. The thickness of the bilayer is less than in TE buffer at 2.7 ± 0.1 nm. The difference in bilayer thickness of DOPE from water and TE buffer may be

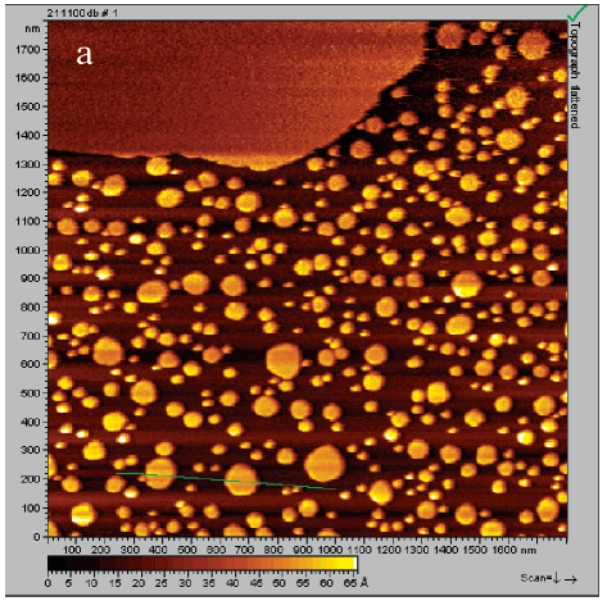

Figure 3. (a) An AFM image of a supported bilayer prepared from a 0.1 mg/mL DOPE solution in TE buffer. Note the regions of vesicle footprints and continuous bilayer. (b) Magnification of the nonbilayer region formed from a higher concentration (0.5 mg/mL) of DOPE in TE buffer. Arrows point to ridges of the DOPE aggregate on the mica surface.

explained by considering headgroup hydration. It has been reported that in going from a dehydrated to a fully hydrated state, the molecular area of the DOPE headgroup changes from 22 to 44 Å^2.[47] An increase of headgroup volume allows freer motion and therefore more potential gauche defects in the hydrocarbon tails. This may change the parallel packing of tails and the formation of structures with reduced bilayer thickness. It is conceivable that the compressed bilayer structure found in the SPBs already exists in the DOPE-containing liposomes.

We will digress briefly to discuss the possible nature of low concentration DOPE solutions. It is unlikely that the putative DOPE vesicles in TE solution result entirely from the pH (7.6). Moreover, we used water and buffer solutions

(42) Mou, J.; Yang, J.; Huang, C.; Shao, Z. *Biochemistry* **1994**, *33*, 9981−9985.
(43) Yip, C. M.; McLaurin, J. *Biophys. J.* **2001**, *80*, 1359−1371.
(44) Jonston, S. J.; Bayerl, T. M.; McDermott, D. C.; Adam, G. W.; Rennie, A. R.; Thomas, R. K.; Sackmann, E. *Biophys. J.* **1991**, *59*, 2889−2894.
(45) Heimburg, T. *Biophys. J.* **2000**, *78*, 1154−1165.
(46) Cullis, P. R.; De Kruijff, B. *Biochim. Biophys. Acta* **1978**, *513*, 31−42.
(47) Rand, R. P.; Fang, Y. *Biochem. Soc. Trans.* **1993**, *21*, 266−270.

of the same pH. The pK_a's of the phosphate and ammonium moieties are known to be approximately 3.5 and 8.0, respectively.[48] If the ammonium was mostly in the deprotonated form, DOPE would become negatively charged and have a much lower propensity to bind to mica. Finally, the stabilization of the sonicated DOPE solution could occur through the formation of lipid fragments.[49,50]

It is curious that the presence of EDTA seems to affect DOPE-containing bilayer properties. A decrease in headgroup hydration could possibly result from a hydrogen-bonding network between the DOPE amine group and the carboxylates of EDTA. EDTA is a well-known chelating agent used to help lengthen the life of DNA solutions by binding divalent cations. Moreover, calculations have suggested that in the L_α phase there is a tendency for the PE headgroup to participate in hydrogen bonding.[51] The EDTA−DOPE hydrogen bonding could prevent the hydration of DOPE headgroups in the SPB and thus restrict the headgroup size. This, in turn, could reduce the tendency of tail gauche defect formation. This fact correlates well with the observed bilayer thickness, 4.5 nm, and the lower fluidity of the bilayer in the presence of EDTA.

We have performed additional experiments (data not shown) where a DOPE bilayer formed from pure water was exposed to a solution of more EDTA (0.5 mM). A disruption of the bilayer is observed resulting in condensed features with very similar striation patterns to those shown in Figure 3b. A simple explanation of this would be an EDTA-induced $L_\alpha-H_{II}$ phase transition on the mica surface. This phase behavior is hypothesized to occur when the headgroup area is smaller than that of the tail, resulting in an inverted cone shape for the phospholipid. More experiments are planned to examine this interesting result, but they are beyond the scope of the current publication.

DPTAP Bilayer. Supported DPTAP bilayers were formed on regular freshly cleaved mica by applying 70 μL of 0.5 mg/mL vesicle solution in water at room temperature. After 20 min, the liquid cell was gently rinsed with water. Supported DPTAP bilayers are in the L_β phase at room temperature and displayed two domains of different heights (5.5 ± 0.2 and 3.8 ± 0.2 nm). These domains showed no changes in defect size or shape during 1−3 h of scanning. Heating the bilayer to 50 °C and then cooling it back to room temperature induced the formation of more domains with reduced thickness. The difference in the thickness of the two domains was 1.7 nm (Figure 4). This is comparable to those observed by Longo and co-workers[32] with the difference between two domains being 1.4 nm. There is some change in the relative proportion of the high and low domains induced by a heating/cooling cycle, again consistent with the previous study.[32] The domains could result from different degrees of chain tilting or interdigitation.

Mixed Supported Phospholipid Bilayers. As can be noted from Table 1, mixed lipid bilayers containing DOTAP and DOPC lead to a thickness intermediate between those of the pure DOPC and pure DOTAP SPBs. This is probably due to DOTAP increasing the average lipid spacing in the mixed membrane. Thus, the DOPC tails may acquire more

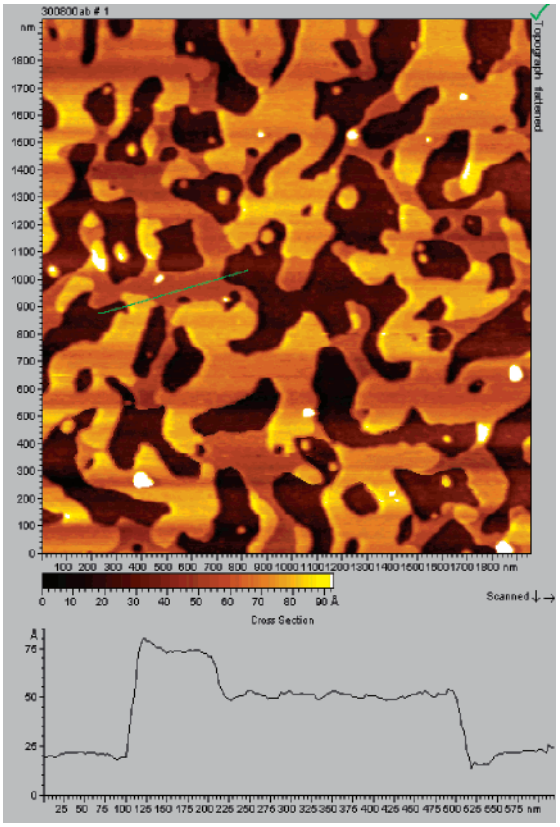

Figure 4. An AFM image of a DPTAP supported planar bilayer on mica imaged in water after heating to 50 °C and then cooling back to room temperature. The image is approximately 2000 nm × 2000 nm. The subpanel is a cross section indicated by the green line in the main panel. The darkest areas are defects in the supported planar bilayers and represent the mica support. Note the evidence of two different height domains in the bilayer.

gauche defects leading to a decreased bilayer thickness compared with that of a pure DOPC bilayer. Our data are in qualitative agreement with DOTAP, DOPC, and DOTAP/DOPC bilayer thickness determined by high-resolution synchrotron X-ray diffraction and show compatible trends when comparing the headgroups.[11] One must note that the values determined from the diffraction study describe the pure bilayer thickness in hydrated multilayer structures and therefore may not represent the exact environment of an SPB.

Mixed DOTAP/DOPE bilayers made from TE buffer solution are the thinnest of all that we have measured in this study. When the lipids are mixed, a cooperative effect seems to take place making the SPB thinner than either bilayer formed from its pure constituents. From Table 1, we note that when formed from TE, DOTAP/DOPE, DOTAP, and DOPE SPBs have thicknesses of 2.4, 3.5, and 4.5 nm, respectively. We also note that the stability of the liposome solution was very sensitive to the solution contents (i.e., EDTA). Recall that only lipid concentrations below 0.1 mg/mL would produce clear EDTA-containing solutions. Moreover, the mixed DOTAP/DOPE bilayer displays anomalous behavior with respect to solution content. It gets thicker as EDTA is removed and as ionic strength is lowered. It may be that DOTAP causes conformational changes in the DOPE headgroup due to electrostatic interactions. These conformational changes would indeed be very sensitive to shielding by water and counterions. Additionally, the cationic surface of the bilayer may attract EDTA, leading to an increase in headgroup volume. Here, since the bilayer is mixed, DOPE−EDTA−DOPE hydrogen bonding may not occur.

(48) Ellens, H.; Bentz, J.; Skoza, F. C. *Biochemistry* **1984**, *23*, 1532−1538.
(49) Madden, T. D.; Cullis, P. R. *Biochim. Biophys. Acta* **1982**, *684*, 149−153.
(50) De Kruijff, B.; Verkleij, A. J.; Van Etcheld, C. J. A.; Gerritsen, W. J.; Mombers, C.; Noordam, P. C.; De Gier, J. *Biochim. Biophys. Acta* **1979**, *555*, 200−209.
(51) Pink, D. A.; McNeil, S.; Quinn, B.; Zuckermann, M. J. **1998**, *1368*, 289−305.

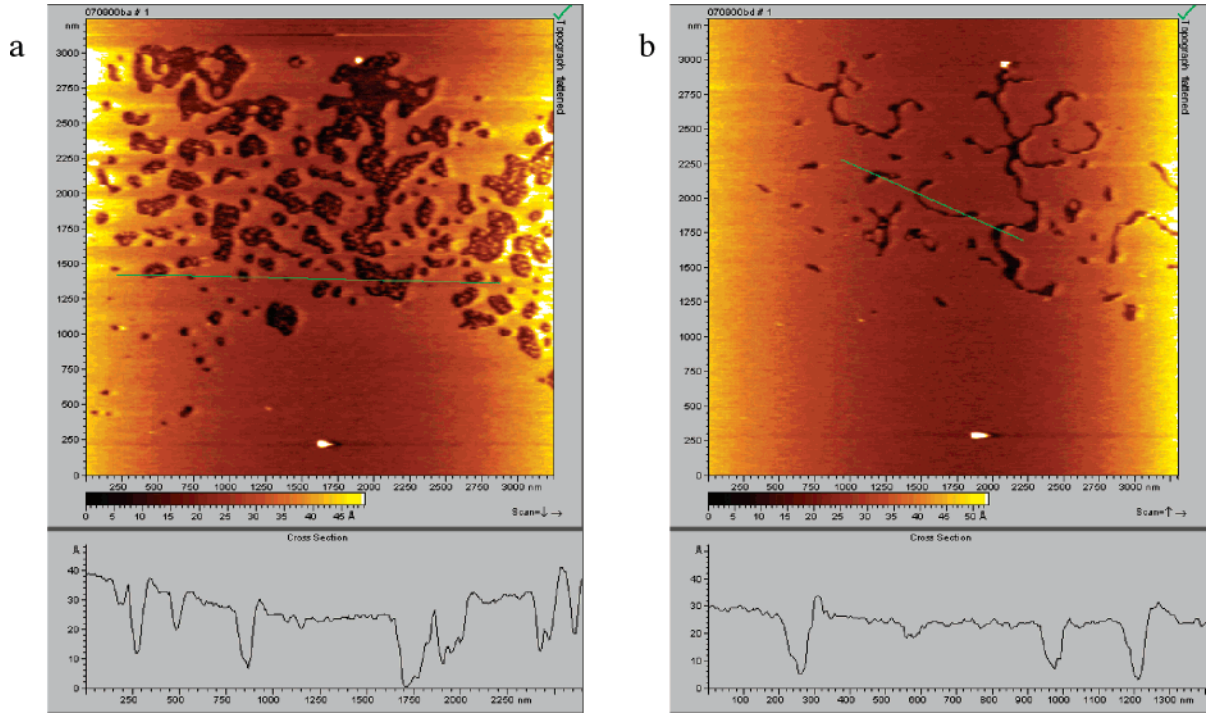

Figure 5. AFM topography images of a DOTAP/DOPE supported bilayer on mica. The SPB was prepared from 5 mg/mL DOTAP/DOPE in water. The image displayed in panel a was collected immediately after rinsing, whereas the image in panel b was collected 1 h after panel a. The subpanels are topographical cross sections indicated by the green lines in the main panels. The images are of the same region and are approximately 3.25 × 3.25 μm.

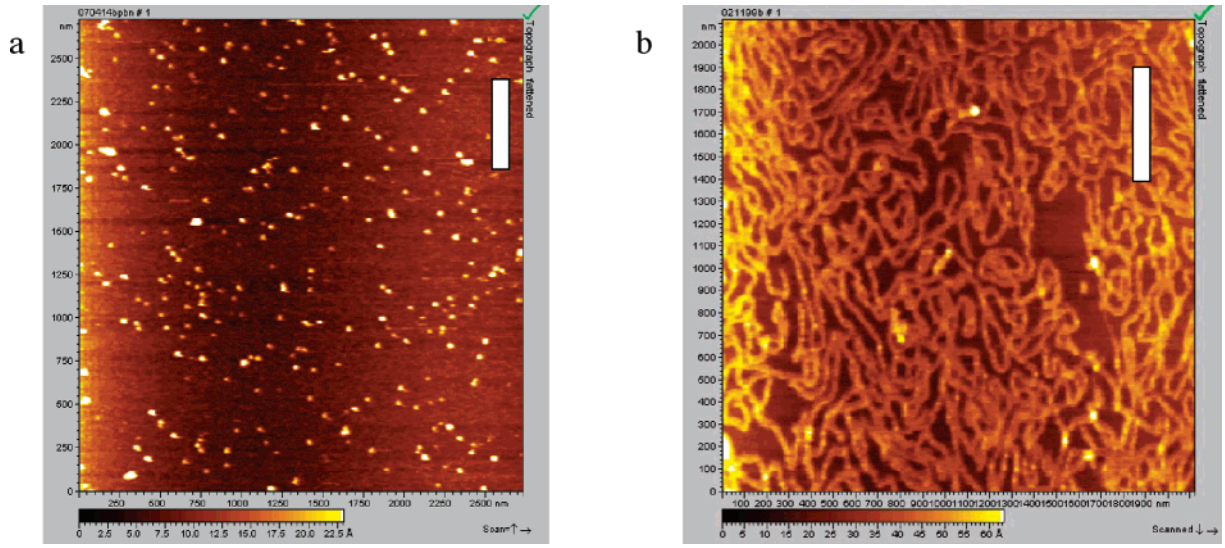

Figure 6. (a) 14 base pair oligodeoxynucleotides (double stranded) on APTES-modified mica. The scale bar on this image is 500 nm. (b) 3000 base pair linearized plasmid DNA bridged onto mica by Mg^{2+}. The scale bars on these images are 500 nm.

Thus, EDTA will not lead to a decrease in DOPE headgroup volume. Electrostatic EDTA−DOTAP interactions may also result in an increased DOTAP headgroup volume. The thinner bilayer displays faster defect-closing dynamics (Figure 5) suggesting that the edges of the EDTA-containing defects are much less stable than for thicker bilayers.

DNA Adsorption. *Adsorption of DNA onto Mica.* Since DNA in TE buffer solution does not bind to regular mica (negative surface charge), the surface was modified with APTES or PLL (positive surface charge). We also used Mg^{2+} ions as binding bridges between DNA and regular mica.[52,53] A height of 2.0 ± 0.2 nm was measured for the 14 base pair oligodeoxynucleotide (ODN) on mica. The image used to calculate this height is displayed in Figure 6a. Small DNA appear as flat ovoids, due to the convolution of the tip radius (∼10−40 nm) onto the surface feature. This results in the width of the DNA being overestimated. The height measurements, however, are not limited by the tip radius and give a better representation of the true DNA diameter on a solid surface. Our data for large DNA adsorbed on a solid mica surface give a height of 2.0 ± 0.1 nm. The AFM image of 3000 base pair DNA on mica is displayed in Figure 6b. Without surface modification or use of Mg^{2+}, no DNA was observed to bind. DNA on mica

(52) Hansma, H. G.; Laney, D. E. *Biophys. J.* **1996**, *70*, 1933−1939.

(53) Han, W.; Dlakic, M.; Zhu, Y. J.; Lindsay, S. M.; Harrington, R. E. *Proc. Natl. Acad. Sci. U.S.A.* **1997**, *94*, 10565−10570.

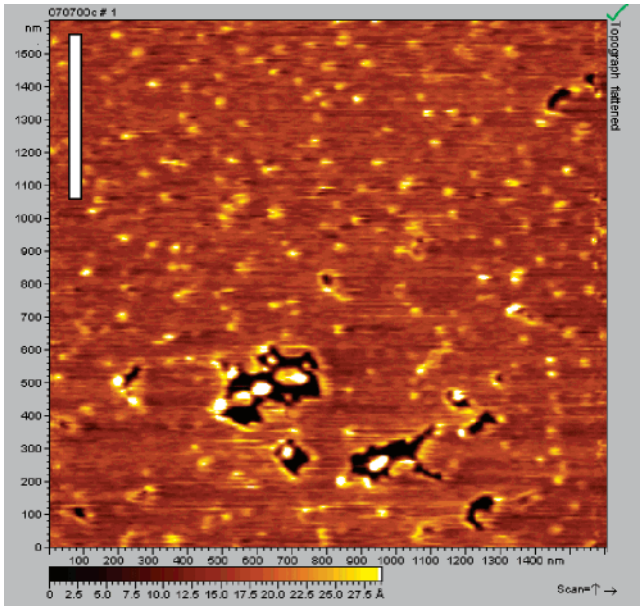

Figure 7. 14 base pair oligodeoxynucleotides adsorbed onto a DOTAP/DOPE supported bilayer. The ODNs appear as ovoid features approximately 1.3 nm higher than the SPB surface. The scale bar on this image is 500 nm.

was also examined at 50 °C and found not to change height compared with room temperature.

DNA on a Supported DOTAP/DOPE Bilayer. When a solution of (2 mg/mL) 14 base pair DNA was exposed to a DOTAP/DOPE SPB for 30 min and then gently rinsed, the oligodeoxynucleotide was found to associate with the surface. When the same solution, devoid of DNA, was exposed to the bilayer, no ovoids were observed. Figure 7 is an example of an AFM image of 14 base pair DNA on a DOTAP/DOPE SPB. One can compare this with the image of the short ODNs on mica (Figure 6a) and note that only the contrast has changed and that there are some defects present in the bilayer. The measured 1.3 ± 0.2 nm height of 14 base pair DNA on a supported planar DOTAP/DOPE bilayer suggests that the ODN is partially buried. There are two possible explanations for the reduction in height. In the first, an AFM tip interaction pushes DNA into the bilayer. The second is that the electrostatic DNA−DOTAP interaction pulls the DNA slightly into the head region of the bilayer. Adsorption of 14 base pair DNA does not appear to disturb the bilayer. Only a few defects were observed after removal of the excess of DNA from the cell. This effect is comparable to rinsing the sample cell with buffer solution containing no DNA. Adsorption of 14 base pair DNA did not change the bilayer thickness.

Interestingly, when 14 base pair DNA was first incorporated onto vesicles by stirring a solution of DOTAP/DOPE and DNA in TE buffer for 30 min, complexes of vesicles with DNA adsorbed to APTES (i.e., positive charge) mica and formed areas of bilayer with a thickness of 4−6 nm. It was found that DOTAP/DOPE vesicles do not bind to APTES mica in the absence of DNA. Thus, preassociation of the DNA with the liposomes appears to promote bilayer formation onto a positive charged surface, possibly with the DNA acting as a bridge.

Unlike 14 base pair DNA adsorption, 1000 base pair DNA adsorption onto DOTAP/DOPE changed the bilayer dramatically; see Figure 8. After addition of 100 μL of 10 μg/mL 1000 base pair DNA (in TE buffer, 20 mM NaCl), partial removal of the bilayer from mica was observed. The remaining SPB also developed domains with different heights ranging from 3.5 to 6 nm. During the time of observation, the higher regions of the bilayer changed, decreasing in area coverage and increasing in height to 7−10 nm. Large DNA (1000, 2880, and 3000 base pair) appears to disrupt the SPB due to formation of large complexes, which easily detach from the mica surface. The bilayer surface coverage changes from 86.9% without DNA to 42.4% when the bilayer is exposed to DNA. This estimation has been made on the basis of averaging 10 different areas. In a control experiment, DNA-free (TE) buffer solution was applied to a supported bilayer. In this instance, no bilayer removal was observed.

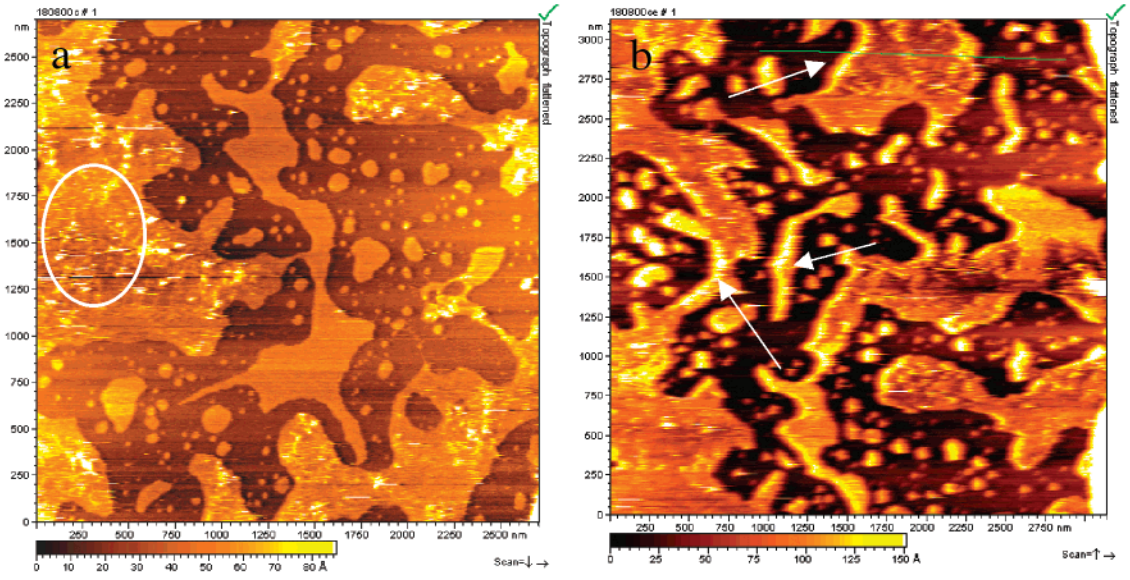

Figure 8. (a) 1000 base pair linearized plasmid DNA adsorbed on a DOTAP/DOPE supported bilayer. The topography image was collected within minutes of exposing the SPB to DNA-containing solution. The oval contains a region with considerable filamentous structure which may represent adsorbed DNA. Note that the bilayer has been significantly disrupted compared to the DOTAP/DOPE SPB in Figure 5. (b) The same sample imaged 1 h after panel a. More disruption is evident, and less DNA is observed. The regions indicated with arrows point to feature edges with height significantly greater than one bilayer. These could be regions of condensed DNA lipoplexes. The scale of the images is 3 μm × 3 μm.

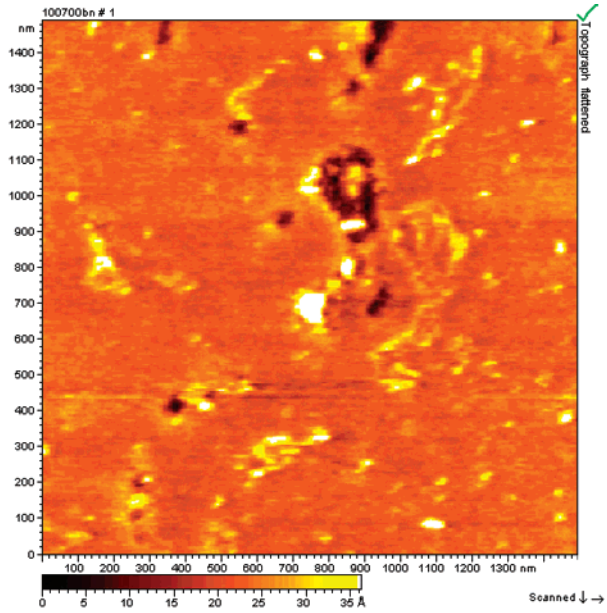

Figure 9. An image of a DOTAP/DOPE bilayer which was exposed first to a 50 μL solution containing 2 mg/mL 14 base pair ODNs for 30 min and then to a 10 μL solution containing 1 mg/mL 1000 base pair linearized plasmid DNA for 10 min.

Additionally, when a lower concentration of 1000 base pair DNA was used the bilayer was not destabilized. The image of DNA−DOTAP/DOPE presented in Figure 9 was stable for many hours. In fact, this image provides the highest contrast of the longer DNA on a fluid SPB. Therefore, there appears to be a critical surface DNA concentration below which the planar lipoplex is stable.

DNA on a Supported DOTAP/DOPC Bilayer. To assess the role of the helper lipid, DOPE, on the above-mentioned behavior, we examined the effect of DNA adsorption to a binary system with a different zwitterionic helper lipid, DOPC. The addition of DNA to the supported DOTAP/DOPC bilayer shows adsorption of DNA at the bilayer surface and partially removes a bilayer from mica, but not as severely as it does for DOTAP/DOPE. No changes of bilayer thickness were observed. Statistical analysis of our data on the height of large DNA adsorbed on a DOTAP/DOPC SPB gives 1.5 ± 0.2 nm. This height is calculated from the elevated features found in Figure 10. In this image, the DNA appear as filamentous features on the bilayer surface. This could arise if the DNA were weaving in and out of the bilayer such that only shorter portions of it are observable. This is compared with images where the entire length of DNA is observable, for example, on mica or gel phase bilayers. Again, control experiments reveal no such filaments when DNA is absent from the preparation.

DNA on a Supported DOTAP Bilayer. As a final assessment of the role DOPE plays in the instability of the mixed SPB, DNA solutions were exposed to a pure DOTAP bilayer. The DNA height was measured as 0.8 ± 0.2 nm (image not shown). This system was stable for a period of hours despite the high fluidity of a DOTAP SPB. The adsorption of DNA did not appear to affect the bilayer thickness. Since DOTAP and DOTAP/DOPC SPBs were more stable to DNA adsorption than the DOTAP/DOPE bilayer, DNA heights could be measured and compared. In these instances, the average heights were 0.8 and 1.5 nm, respectively, and are consistent with the extreme fluidity of the DOTAP bilayer and lower fluidity of the DOTAP/DOPC bilayer and with both of the hypotheses that DNA is either pulled into the bilayer electrostatically

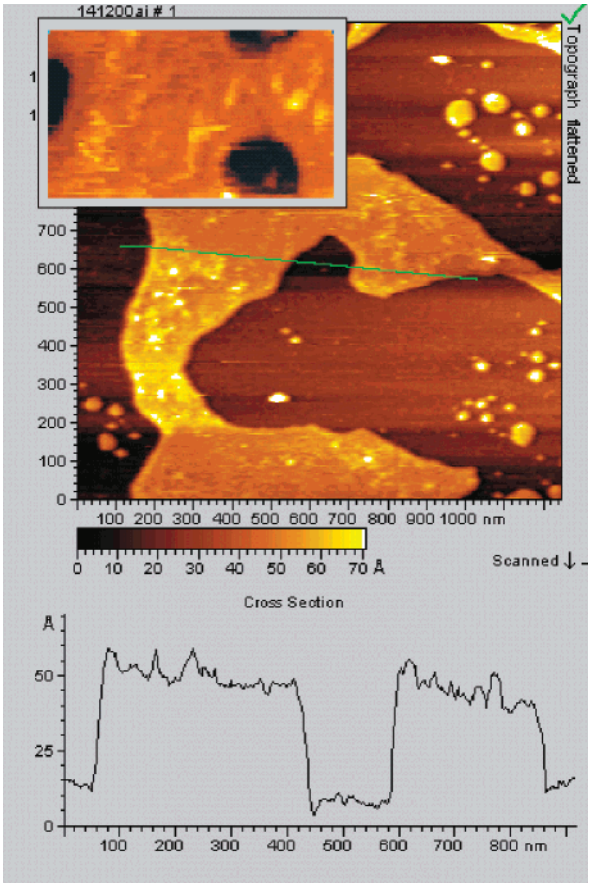

Figure 10. 1000 base pair linearized plasmid DNA adsorbed onto a DOTAP/DOPC supported bilayer. The subpanel is a topographical cross section indicated by the green line in the main panel. The inset is a digital zoom of a region with evidence of adsorbed DNA.

or pushed in by the AFM tip. We are confident that a minimal tip-related force is exerted on the adsorbed DNA, because we never observed evidence of the tip displacing or dislodging DNA during a scan. It is therefore more likely that the DNA is naturally buried in the bilayer, compounding the challenge of its detection with AFM. The 1.5 nm height of DNA on DOTAP/DOPC may suggest that in this system, DNA encounters the higher DOPC headgroups at the bilayer interface, although it is still bound to the SPB by electrostatic interactions with DOTAP. Interestingly, when surface plasmon spectroscopy (SPS) was used to investigate DNA−DOTAP interactions on an alkylthiol supported bilayer,[40] a DNA height of 0.5 nm was reported. Since SPS is not noninvasive, this suggests that cationic bilayers in the liquid phase could allow penetration of DNA into the headgroup region. The authors suggested that this unexpectedly low height was due to incomplete packing of DNA onto the bilayer surface. However, our measured height of 0.8 ± 0.2 nm is in nice agreement with their result suggesting that they may indeed have measured the true thickness of a DNA layer on a liquid phase bilayer.

DNA on a Supported DPTAP Bilayer above and below the Phase Transition Temperature. As we have shown recently, DNA adsorbed on a bilayer can be observed during heating above the transition temperature.[29] To examine the dependence of DNA height on the lipid phase, we monitored the temperature dependence of the DNA−DPTAP system to provide corroboration of our other DNA−CL (L_α) images. Adsorption of linear 3000 base pair DNA on top of a DPTAP SPB is shown in Figure 11. DNA

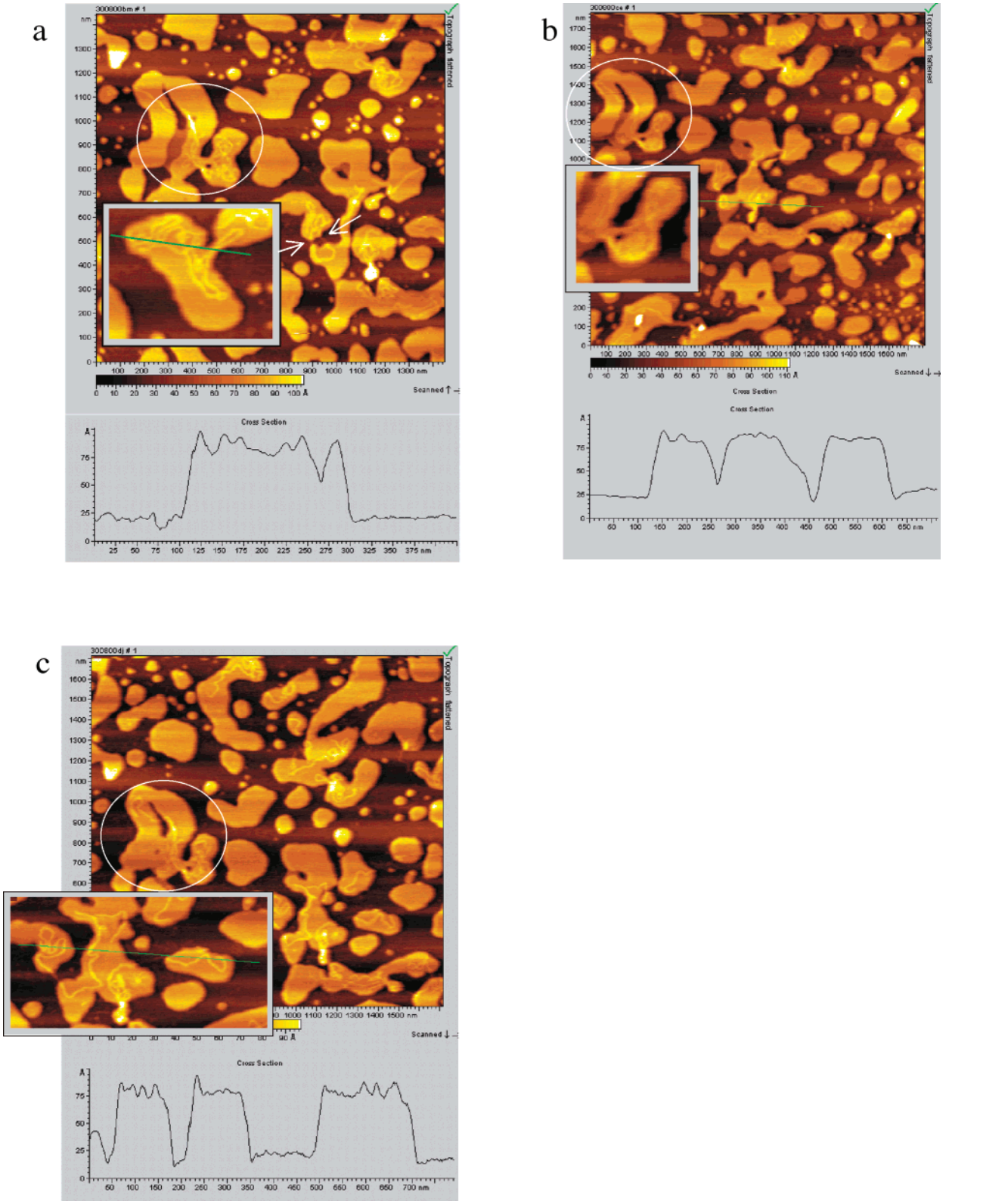

Figure 11. AFM images of DNA on a DPTAP bilayer as a function of temperature. The darkest areas represent the mica substrate. Bright filaments represent DNA adsorbed onto the bilayer. Note the white oval, which identifies a common surface feature apparent in all scans. The inset images are digitally zoomed DNA-containing areas from the corresponding panels. (a) Recorded at room temperature (approximately 22 °C). The white arrows indicate a feature which may represent DNA bridging two separated bilayer regions. (b) The same sample heated to 50 °C. (c) The same sample after cooling back to room temperature. The insets are digital zooms of DNA-containing regions. The subpanels are topographical cross sections indicated by the green lines in the main panels.

molecules were randomly distributed and well resolved on the surface and are found to adsorb preferentially on the surface of the higher domains. Remarkably, some DNA appears to bridge the gap between separated bilayer areas (see small arrows in Figure 11a). Our result for DNA height adsorbed on gel phase DPTAP is 1.7 nm above the bilayer. Heating the bilayer and cooling it back to room temperature changes measured DNA height to 0.7 ± 0.2 nm at 50 °C and 1.6 ± 0.2 nm at room temperature. From the inset (Figure 11b), it is significant that above the DPTAP

phase transition temperature, the DNA features have become more filamentous. After slow cooling, the contrast and resolution of DNA were restored (Figure 11c). Our results are consistent with those of Fang and Yang,[27] who report a DNA height of 2 nm above a DPDAP bilayer at room temperature. Additionally, others[28] report a DNA height of 1.7 nm above a DPTAP SPB. Both of these studies employed lipids that were in the L_β phase. Significantly, Zantl et al.[54] have investigated the structure of DMTAP/DMPC at temperatures above and below the (L_β−L_α) phase transition using wide- and small-angle X-ray diffraction. They suggested that the presence of DNA might affect the tilting of lipids in the gel phase.

Imaging while scanning temperature for a system like this is not trivial, because changes in the system of study are accompanied by changes in scanning probe properties. The force set point needs constant readjustment during heating to maintain good image quality. Moreover, because we observed a low contrast and resolution of DNA adsorbed on the surface of our L_α phase DPTAP bilayers, one might suggest that this low resolution results from a temperature-induced tip artifact. The comparison of the results for L_α bilayers with those for L_β phase bilayers helped to show that low resolution of adsorbed DNA comes from the difference in the bilayer phase. The change in measured DNA height between gel and liquid phase DPTAP can be compared to the change in bilayer thickness over the same temperature range (see Figure 11a−c cross sections); the image of the bilayer remains relatively stable over the entire temperature range regardless of whether DNA is adsorbed. Moreover, the bilayer itself does not significantly change thickness during heating and cooling. The thickness of the DPTAP bilayer at 50 °C was 5.5 ± 0.3 nm, the same as at room temperature. Additionally, the image contrast and resolution of the DPTAP bilayer at elevated temperature does not decrease. The images found in Figures 8−11 all display the same filamentous regions regardless of the source or type of DNA. These filaments have the appropriate heights for DNA weaving in and out of the top leaf of the bilayer. Taken together, these results provide strong evidence that the change in measured DNA height and image contrast/resolution comes from the fluidity of a L_α phase bilayer supporting the DNA. Thus, we are confident that the filamentous features at heights of 0.7−1.3 nm above the room-temperature L_α phase bilayers are indeed DNA.

General Discussion of SPB Disruption: *Effect of DNA Length and Phospholipid Type.* Adsorption of small 14 base pair ODNs onto a DOTAP/DOPE bilayer does not produce any extra defects on the surface. Any bilayer distortions caused by the adsorbed oligomers therefore must be easily neutralized by phospholipid readjustment. From Figure 8, it is clear that larger DNA molecules do not interact with the bilayer in the same manner as 14 base pair ODNs. Larger DNA removes a DOTAP/DOPE bilayer from the surface due to formation of large complexes, which presumably detach and return to solution.

From our results, we know that a DOTAP/DOPE bilayer is very mobile. Moreover, this mixed bilayer possesses the ability to transform to the hexagonal phase.[10,39] During the electrostatic interaction of a DOTAP/DOPE bilayer with DNA, positively charged DOTAP lipids likely migrate to DNA in order to neutralize the negative charge of DNA and neutral phospholipids must concomitantly move away.

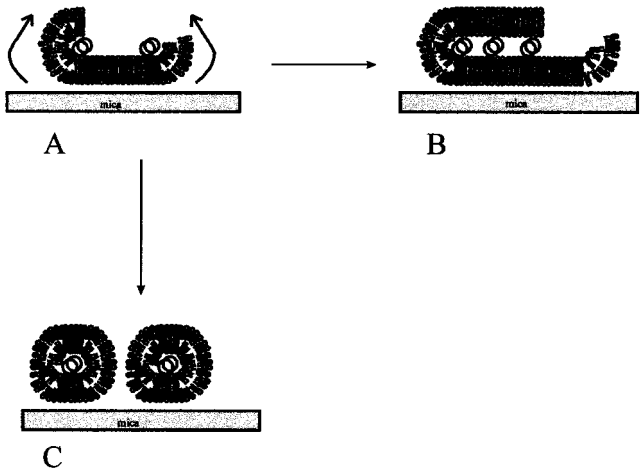

Figure 12. (A) The schematic diagram of a vertical slice through DNA (barrels) adsorbed onto and disrupting a bilayer. (B) A possible lamellar sandwich structure of a DNA-disrupted supported bilayer. (C) A hexagonal phase wrapping of DNA possibly leading to desorption of the lipoplex from the surface.

This phenomenon was described previously.[17,55] A lipid demixing process can change the elasticity of the membrane with respect to stretching and/or bending deformations. Therefore, the presence of DNA can result in lipid sorting, which leads to distortion in the metastable bilayer by regions rich in DOPE. This may allow a lamellar to hexagonal phase transition to take place incorporating the DNA, as schematically diagrammed in Figure 12. Indeed, this inverted hexagonal structure has proven to be the most stable in aqueous solution both experimentally[10] and theoretically.[6] Thus, SPB destabilization may ultimately lead to desorption of lipoplexes from the surface.

From Figure 8, recall that for large DNA on a DOTAP/DOPE bilayer, we observed regions with a height 1−2 nm greater than that of a double bilayer, that is, a total height of 7−8 nm. This may indicate that DNA is sandwiched either by a lamellar bilayer as shown in the schematic Figure 12B or by an inverted hexagonal packing as suggested in Figure 12C. Additionally, we have observed that regions of single bilayer thickness decrease with time for adsorption onto DOTAP/DOPE. This is likely due to conversion into a more condensed phase and is consistent with the idea that the inverted hexagonal phase is the most stable.[6,10] Note that at the edges of the bilayer area (see arrow in Figure 8), the height is greatest suggesting a potential rolling of the lipid around the DNA.

Neither DOTAP/DOPC nor pure DOTAP bilayers display a propensity for severe distortion when they interact with DNA. DNA binds to the DOTAP/DOPC SPB and partially removes the bilayer from mica, but much less extensively compared with DOPE-containing SPBs. Thus, for a DOTAP/DOPC bilayer, the lamellar form is the most stable and bending of the bilayer cannot be significantly induced by DNA. This is consistent with the negligible spontaneous curvature of the helper lipid DOPC.[10,19] The same is true for pure DOTAP−DNA interactions, because DOTAP also has a zero spontaneous curvature.

Compared with the previous studies following the binding of DNA to L_β phase SPBs,[27,28] we do not observe the same exclusively tight packing of DNA. This is regardless of incubation times, which were as long as 24 h. It is plausible that this is because we did not use divalent

(54) Zantl, R.; Artzner, F.; Rapp, G.; Rädler, J. O. *Europhys. Lett.* **1998**, *45*, 90.

(55) May, S.; Harris, D.; Ben-Shaul, A. *Biophys. J.* **2000**, *79*, 1747−1760.

cations or excess EDTA, which have been shown to promote close packing of DNA on bilayers.[18,27,28]

Perhaps the most striking observation in this work is the dependence of a DNA-induced DOTAP/DOPE $L_\alpha-H_{II}$ phase transition on the DNA length. DNA of length 14 base pairs does not induce this transition, whereas DNA of 1000 base pairs and longer does. Elegant calculations of this phenomenon[6] were performed by May et al. assuming DNA to be a rigid rod of uniform charge density. In their work, the authors note that the most important factor for inducing a $L_\alpha-H_{II}$ phase transition is an approach to isoelectricity, that is, a charge balance between the cationic phospholipids and the polyanionic DNA. This isoelectric point likely occurs spontaneously on an SPB surface in the presence of adsorbed DNA, since this is the point of lowest free energy.[6] For longer DNA, the approximation of May et al. holds well, but for shorter DNA well dispersed on the SPB surface, the groove structure and discrete distribution could be significant. Also, the entropic energy price of reorganizing the lipids at the ends of the short DNA may compensate the electrostatically driven free energy gain in the phase transition. Since the aspect ratio is vastly greater for the longer DNA, its ends can be neglected in the phase transition process.

Conclusions

The process of creating liposomal vehicles for gene delivery involves the association of cationic lipids and DNA to form a lipoplex. The formation and stability of the lipoplexes depend on many factors including lipid composition, that is, the types of cationic and helper lipids used.[6] The incorporation of the helper lipid, DOPE, leads to severe disruption of the supported planar bilayer by DNA, presumably due to the DOPE negative radius of curvature. Moreover, we have helped to elucidate stages in the process of complexation at the single DNA level. By melting gel phase bilayers with adsorbed DNA, we have shown that the contrast, the resolution, and the measured height of adsorbed DNA depend on the bilayer phase. Further experiments are planned to confirm demixing and phase transformation processes as elementary steps in the mechanism of DNA−CL complexation.

Acknowledgment. This work was financially supported by NSERC (D.T.C.), the Alberta Cancer Board (SPL-M, D.T.C.), the National Cancer Institute of Canada (SPL-M), Travis Chemicals (a Division of Stanchem (Calgary)), and the University of Calgary. The continued support of Molecular Imaging is also gratefully acknowledged. The authors thank Professors R. Epand and P. Cullis for helpful discussions.

LA0116239